JOURNAL OF PROPULSION AND POWER
Vol. 9, No. 3, May–June 1993

Commercial Turbofan Engine Exhaust Nozzle Flow Analyses

Khaled S. Abdol-Hamid*
Analytical Services and Materials, Inc., Hampton, Virginia 23666
K. Uenishi† and B. D. Keith†
ATO/General Electric Aircraft Engines, Cincinnati, Ohio 45201
and
John R. Carlson‡
NASA Langley Research Center, Hampton, Virginia 23681

The recently developed three-dimensional code is able to perform a computational investigation of complex aircraft aerodynamic components. This code was developed for solving the simplified Reynolds-averaged Navier-Stokes equations in a three-dimensional multiblock/multizone structured mesh domain. The present analysis was applied to commercial turbofan exhaust flow systems. Solution sensitivity to grid density is presented. Laminar flow solutions were developed for all grids, and two-equation k-ε solutions were developed for selected grids. Static pressure distributions, mass flow, and thrust quantities were calculated for on-design engine operating conditions. Good agreement between predicted surface static pressures and experimental data was observed at different locations. Mass flow was predicted within 0.2% of experimental data. Thrust forces were typically within 0.6% of experimental data.

Nomenclature

A_t = nozzle throat area, cm^2
F = total vector thrust, N
Fi = ideal isentropic gross thrust, N
f = incremental vector force of a computational cell
n = unit normal vector
p = static pressure, Pa
p_t = total pressure, Pa
P_∞ = freestream static pressure, Pa
R = gas constant (γ = 1.4), 287.3 J/kg-K
r = reference length, cm
U = total velocity vector, m/s
w_i = ideal mass flow rate, kg/s
w_p = calculated mass flow rate, kg/s
ρ = density, kg/m^3

Introduction

Design Considerations

ACHIEVING an aerodynamic contour design that meets performance specifications for a modern high-bypass-ratio turbofan engine, involves complex, time-consuming, and expensive analysis and testing. A great deal of this effort is expended on designing aerodynamic contours for exhaust system components (fan nozzle, core nozzle, plug, etc.) that efficiently satisfy operating conditions both on- and off-design. The fundamental purpose of the exhaust system is to discharge the exhaust gases to the ambient pressure with the highest possible axial thrust at the cruise design condition. This requires exhaust designers to size the fan and core nozzle throats to ensure passage of the flow rate required by the engine cycle with minimum pressure loss and minimum external drag. In the actual design process, however, the mechanical constraints of the system may compromise the optimal aerodynamic shapes. A more detailed discussion of design issues associated with the exhaust system can be found in Refs. 1 and 2.

Generally, exhaust systems for high-bypass turbofan engines may be classified as separate flow or mixed flow, as schematically shown in Figs. 1 and 2, respectively. This article will focus on the exhaust system only, neglecting the inlet portion of the engine. The exhaust nozzle system can be further simplified with an assumption of axisymmetric geometry if the upper bifurcator/pylon and lower bifurcator are ignored. However, the upper and lower bifurcators strongly influence the exhaust nozzle flowfields, and can significantly affect the engine installed performance. Therefore, discussion in this article will be limited to only full three-dimensional analysis, even though the axisymmetric exhaust aerodynamic analysis can provide some meaningful insights during the design process.[3] Furthermore, the installation of an exhaust system on an aircraft has a significant impact on the exhaust system performance. Present CFD capabilities have advanced to the point of being able to analyze flowfields of the installed exhaust system under a wing.[4] However, for applications of CFD to exhaust system design, current computational resources somewhat limit the analysis to the isolated exhaust system. The present work, therefore, is focused on the isolated exhaust system design.

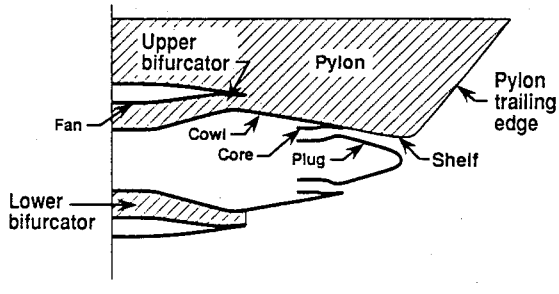

Fig. 1 Exhaust aerodynamic components (separate flow).

Received May 6, 1992; presented as Paper 92-2701 at the AIAA 10th Applied Aerodynamics Conference, Palo Alto, CA, June 22–24, 1992; revision received Oct. 6, 1992; accepted for publication Dec. 9, 1992. Copyright © 1992 by the American Institute of Aeronautics and Astronautics, Inc. No copyright is asserted in the United States under Title 17, U.S. Code. The U.S. Government has a royalty-free license to exercise all rights under the copyright claimed herein for Governmental purposes. All other rights are reserved by the copyright owner.

*Senior Scientist. Member AIAA.
†Engineer. Member AIAA.
‡Aerospace Engineer, Propulsion Aerodynamics Branch, Applied Aerodynamics Division. Senior Member AIAA.

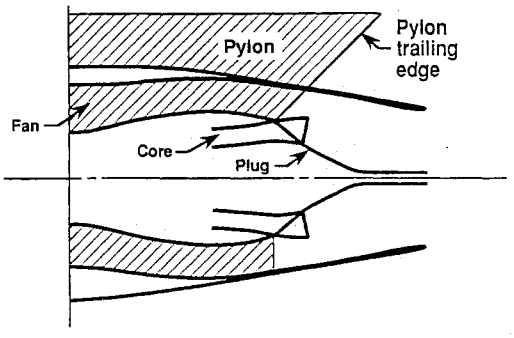

Fig. 2 Exhaust aerodynamic components (mixed flow).

Computational Considerations

A relatively large number of analytical and computational methods for predicting the flowfield surrounding a turbofan engine exhaust system have been developed.[5-9] These methods include computational techniques based on two- and three-dimensional and general Euler equations[5-8] and Navier-Stokes equations.[9] Even though these computational methods are well documented in general publications, they have not been fully transferred into, or accepted by, the design community due to difficulties associated with grid generation, lack of validation, and the requirements that the user possesses substantial computer and computational expertise.

To remove the above-mentioned difficulties, the second and fourth authors (Uenishi and Keith) established a CFD-based turbofan exhaust flowfield analysis system. As described in Ref. 3, this system can assist the designer in the evaluation and pretest screening of candidate designs quickly and efficiently, and lead to a reduction in the total number of necessary test configurations.

This three-dimensional turbofan exhaust nozzle aerodynamics analysis system (ENS3D) is based on the CFL3D code,[10] which includes the algebraic Baldwin-Lomax turbulence model. Due to the complexity of the exhaust flowfield, it has been hypothesized that a better turbulence model would improve the quality of flow and performance predictions. In this article, an improved version of PAB3D code,[11,12] developed by the first author (Abdol-Hamid), is tested and validated utilizing a recently developed k-ε turbulence model.[12] In addition to flowfield analysis, the third author (Carlson) has developed a nozzle performance package which is used to estimate the nozzle performance quantities.[13,14]

Performance

The performance package implemented in the present code has been shown to be capable of calculating mass flow, moment, and force characteristics for single-stream nozzles such as axisymmetric Stratford choked, slotted axisymmetric,[13] axivectoring nozzles, and two-dimensional C-D nozzles with and without thrust vectoring.[14] Mass flow has matched experimental data within a 0.5% or better error band for most of the past case studies. Predicted moments and forces have typically been within 1–2% of experimental data, except for flow conditions that have resulted in large regions of separated flow within the nozzle. In those situations, the predicted forces have been up to 5–10% off for the laminar flow solutions.

The separate flow nacelle studied in this investigation required only minor modifications to the present program to properly account for the forces developed. This is due to the fact of the multiple separate streams not directly interacting before developing their respective momenta characteristics. The lack of a single originating stream of total pressure and temperature for the mixed flow nacelle required the development of an additional module for the determination of the flowfield quantities needed for the ideal mass flow and ideal thrust. The typical approach is through the ideal thermodynamic mixing of the fan and core streams to construct an equivalent stream of total pressure and temperature. This approach should prevent thrust ratios greater than unity.

Computational Procedure

Solver and Boundary Conditions

In the present study, turbofan engine exhaust flowfield contained both subsonic and supersonic regions, with the possibility of flow separation. The present code contains several options for solving the governing equations, including van Leer, Roe, and space-marching scheme. The Roe scheme with third-order accuracy was used in evaluating the explicit part of the governing equations. The van Leer scheme, with its faster convergence rate, is used as the implicit operator. p_t and the total temperature T_t were specified at the inflow faces of the core and fan ducts. An extrapolation boundary condition was applied at the downstream outflow face of the computational domain. A Riemann invariant condition was applied to the upstream far field and outer computational boundaries. Although several turbulence models are available as options, only the k-ε turbulence model was found suitable for the complex configuration considered in the present investigation. The near-wall model of Jones and Launder[15] is used for the flow regions near the solid surfaces.

Aeroperformance Analysis

Nozzle performance was obtained through the application of the momentum theorem to a control volume surrounding the nozzle. The surface over which the integration of the flow quantities is performed is typically the nozzle exit face and some exterior solid surfaces. The actual mass flow and thrust and moment vectors are defined by Eqs. (1) and (2):

$$w_p = \Sigma(\rho \boldsymbol{U} \cdot \hat{n}) \Delta A \tag{1}$$

$$\boldsymbol{F} = \Sigma \boldsymbol{f} \tag{2}$$

where

$$f = [\rho \boldsymbol{U}(\boldsymbol{U} \cdot \hat{n}) + (p - p_\infty)\hat{n}]\Delta A$$

ΔA is the outflow area attributed to the incremental cell face. The nozzle mass flow, w_p, was determined by the average of the mass flow through several cross-sectional grid planes in a flow volume. These planes are chosen in sections of the nozzle duct that show a relatively constant mass flow rate. One of the several criteria for determining convergence was a less than 0.2% deviation in mass flow through the sampled planes. Typically, 10 planes are surveyed for the duct average mass flow. Theoretically, all the cross sections of a given duct should be flowing at the same mass rate, but numerical errors due to insufficient grid density in relation to changing internal geometry can cause locally poor mass conservation. A plane with a mass flow more than 0.2% from the average would be considered poor. Despite local losses of up to 0.2%, overall mass-flow loss (inflow boundary to outflow boundary) has been typically less than 0.05%.

Ideal mass-flow rate and thrust are determined from the isentropic flow Eqs. (3) and (4), respectively, and are used to normalize the calculated mass-flow rate and thrust for comparisons with the experimental data:

$$w_i = \sqrt{\frac{\gamma}{R}} \frac{2}{\gamma + 1}^{[(\gamma+1)/2(\gamma-1)]} A_t \frac{p_{t,j}}{\sqrt{T_{t,j}}} \tag{3}$$

$$F_i = \sqrt{\frac{2\gamma R}{\gamma - 1}} w_p \sqrt{T_{t,j}\left[1 - \left(\frac{p_\infty}{p_{t,j}}\right)^{(\gamma-1)/\gamma}\right]} \tag{4}$$

The performance package permits monitoring of performance parameters as the solution develops. Previous studies[14]

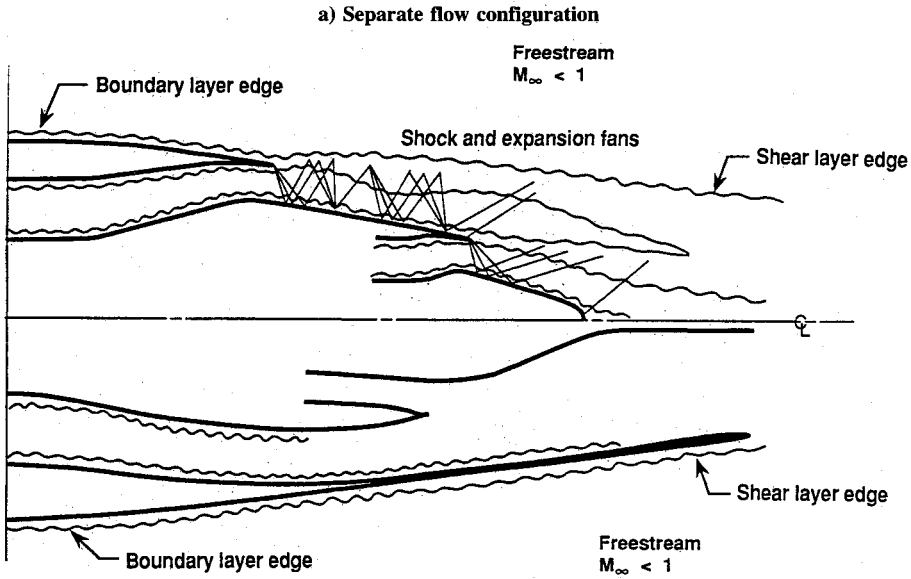

Fig. 3 Flowfield characteristics/turbofan exhaust system.

have shown the need for additional indicators of solution convergence besides the solver residuals. Solution trends of the mass-flow rates and total thrust were utilized in this investigation for convergence evaluation.

The performance of separate flow exhaust systems can be calculated by several methods. In this investigation, total system thrust was determined by the summation of the integrated momentum flux and pressure forces across the fan and core nozzle exits, and the pressure and skin friction forces on the core cowl, pylon, and centerbody washed by the exhaust flows.

The calculation of performance for the mixed flow exhaust system required a modification to the present methodology. For the separate flow nozzle, inflow parameters associated with each stream were used to determine the ideal flow conditions of each stream. The mixed flow nacelle has no a priori ideal parameters for the determination of ideal mass flow and thrust. There exists two choices for these parameters when dealing with the mixing of two streams of differing total pressure and temperatures into a common duct.

An ideal thrust can be determined for each stream individually and summed for a total ideal system thrust. Due to the nature of mixed flow systems, i.e., the mixing of the two streams can result in thrust greater than the two separate streams linearly added. This does not pose a problem if it is recognized that it is a result of the normalizing factor. Alternatively, a more rational approach is to calculate a set of inflow parameters that would serve as an ideal equivalent single-stream feeding the exhaust nozzle system. This can be accomplished by solving the one-dimensional mixing problem of the two streams that differ in total pressure and temperature. This is the one technique utilized to reduce experimental test data.

The thrust generated by the exhaust system is calculated through integration of the efflux at the exit face of the nacelle. The inflow faces of the core and fan were surveyed for the parameters required for the determination of the equivalent ideal single-stream flow parameters (i.e., momentum flux, pressure, velocity, and temperature). The mass-flow rate for the complete configuration was determined by the average of the mass-flux across several grid planes upstream of the nacelle exit.

Results and Discussion

Two nacelle-pylon configurations were considered for comparison of predicted surface pressure coefficients and nozzle performance with experimental data. Laminar and turbulent (k-ε) flow calculations are presented and compared with experimental data. The two configurations considered were the separate flow and mixed flow nacelle/pylon combinations shown in Figs. 1 and 2. The flowfield characteristics for both configurations are shown in Fig. 3. The effect of grid density variations and the effect of flow turbulence modeling are discussed for the separate flow nacelle configuration.

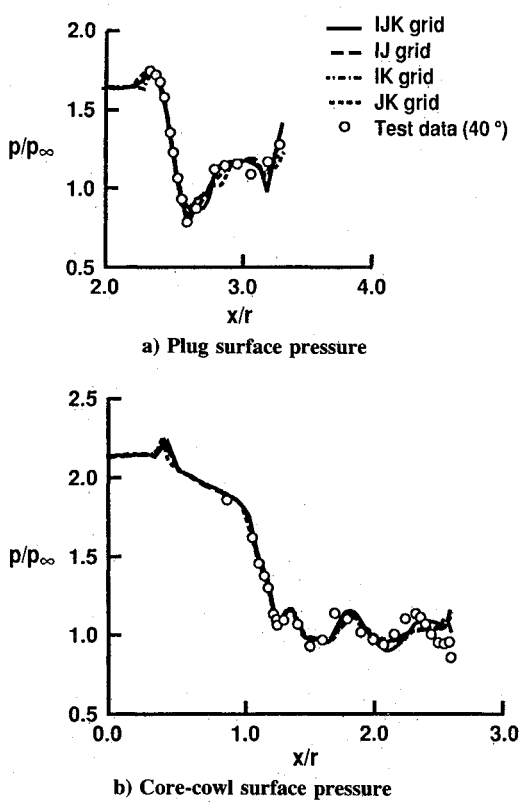

Fig. 4 Pressure comparison for separate flow turbofan (grid study).

Separate Flow Nacelle-Pylon Configuration

Separate computational blocks were used to model the core, fan, and external flowfields. The core and fan blocks extend

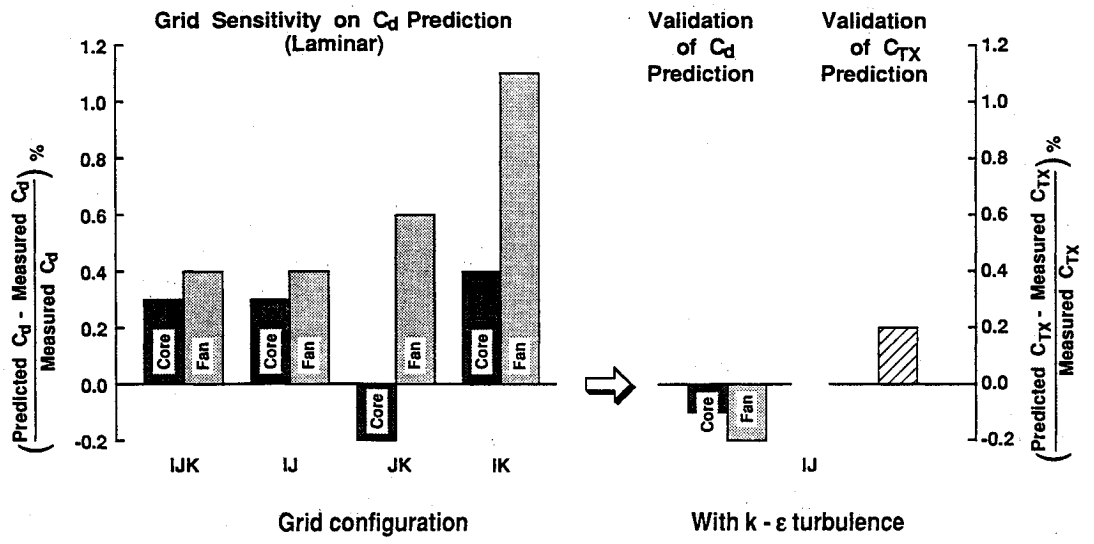

Fig. 5 Comparisons between measured and predicted discharge coefficient (C_D) for separate flow configuration.

from the upstream inflow plane to the downstream outflow plane of the computational domain. The external flow block extends from an upstream freestream inflow plane to the downstream outflow plane, and extends radially out to an outer freestream boundary. A no-slip wall boundary condition is used on all solid surfaces except for the pylon, and upper and lower bifurcator surfaces. Slip boundary conditions were applied to these surfaces due to the lack of proper grid density modeling the viscous effect over those surfaces.

Four computational meshes were used to study the effect of grid density on the prediction of surface pressures and nozzle performance using the laminar flow solution option (which is at least 20% faster than turbulent solution). These grids are designated as IJK, IJ, IK, and JK as follows:

Grid	Block 1	Block 2	Block 3
IJK	89 × 20 × 25	137 × 16 × 25	127 × 16 × 25
IJ	89 × 20 × 49	137 × 16 × 49	127 × 16 × 49
IK	89 × 39 × 25	137 × 31 × 25	127 × 31 × 25
JK	177 × 20 × 25	273 × 16 × 25	253 × 16 × 25

Figure 4 shows the comparison of laminar flow results with experimental data for static pressure coefficients along the plug and core cowl surfaces. These data are along a streamwise row 40 deg from the top centerline, viewing the model from the aft end. Figure 4 shows that the laminar solutions are very good in predicting the plug and cowl surface pressure distributions for all four grid densities. However, the larger number of k cells with the IJ grid, lowering the grid y^+ to less than four (based on turbulent skin friction calculation), appears to be more accurate than the other coarse solutions. This level of y^+ is quite reasonable for k-ε solutions.

Figure 5 shows the relative levels of predicted discharge coefficient for each of the four grid densities. Typically, the laminar solutions predicted slightly higher mass flows as compared to the experimental data (except the core mass flow for the JK grid). The core mass flow was within 0.5% of the experimental level for all the grids. The higher fan mass-flow discrepancy could be due to the lack of boundary-layer grid modeling along the pylon surface washed by the fan flow. The k-ε solutions for the IJ grid accurately predicted the core and fan discharge coefficients to within 0.2% of the experimental data (Fig. 5).

Surface pressure distributions on the plug, cowl, core, and shelf are compared with the experimental data shown in Fig. 6. All the data are measured at 40 deg from the top centerline, viewing the model from the aft end, except the shelf data is measured under the pylon. In general, both the laminar and turbulent solutions match the experimental data on these sur-

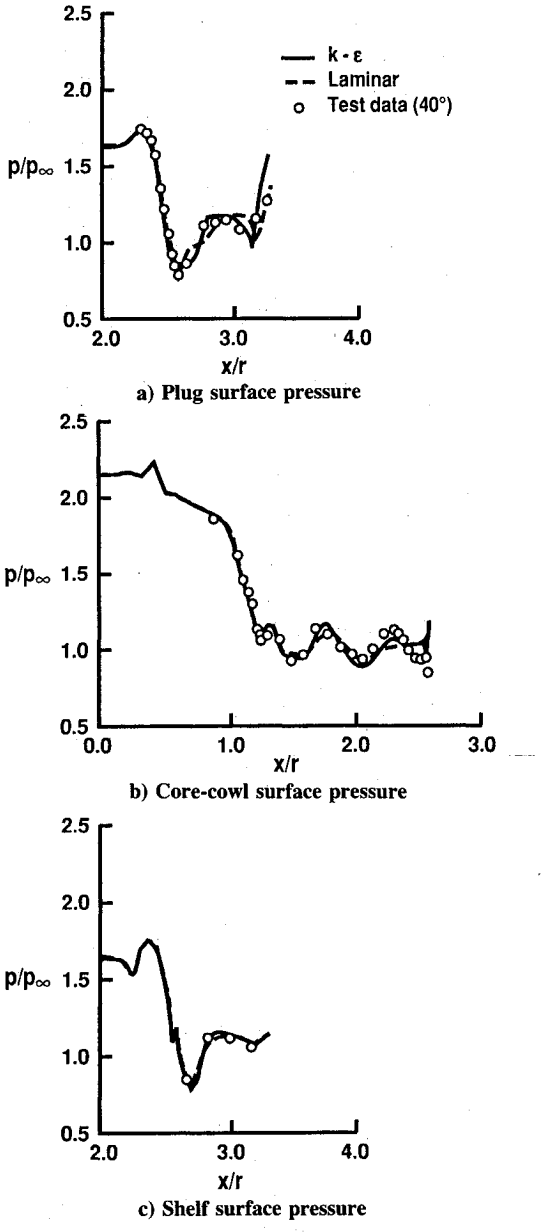

Fig. 6 Pressure comparison for separate flow turbofan (laminar and k-ε solutions).

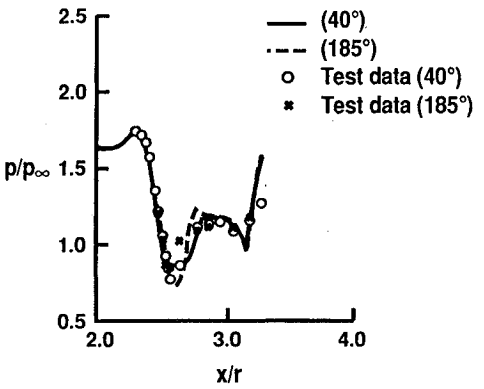

a) Plug surface pressure

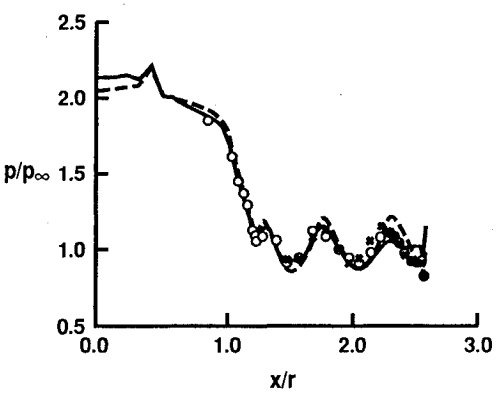

b) Core-cowl surface pressure

Fig. 7 Pressure comparison for separate flow turbofan (k-ε solutions).

faces fairly closely. However, the turbulent flow solution was slightly better than the laminar solution, particularly when comparing the shelf and cowl surface pressure distributions. This improvement is likely due to the k-ε turbulence solution predicting a much thicker shear layer at the exit of the fan duct as compared with laminar results. This results in a more realistic pressure field for the fan and core streams to recover into.

Predicted pressure distributions at two sector angles, 40 and 185 deg, are compared with experimental data in Fig. 7. The nonaxisymmetric flow of this nacelle is accurately predicted by the IJ grid k-ε solution. At 185 deg, some of the pressures on the plug and core-cowl surface are slightly higher than similarly streamwise-located pressures along the 40-deg sector. These pressure variations are the effect of the pylon surface on the flow development inside both the core and fan ducts.

Mixed Flow Nacelle-Pylon Configuration

As with the separate flow nacelle computational domain structure, separate blocks were used for each of the flow streams. The three blocks used in the present study were dimensioned 125 × 31 × 49, 165 × 31 × 49, and 81 × 31 × 49 for the core, fan, and external flow regions, respectively.

A comparison of laminar and turbulent flow pressure distributions with experimental data along the inner fan surface are shown in Fig. 8. The two predicted pressure distributions were practically identical and closely matched the general trend of the data. The k-ε solution predicted the total mass flow of the mixed-flow exhaust system to better than 0.1% of the experimentally measured level, as shown by the bar chart in Fig. 9. The predicted axial thrust level, as was the predicted ratio of fan-to-core mass flow, was roughly 0.6% high.

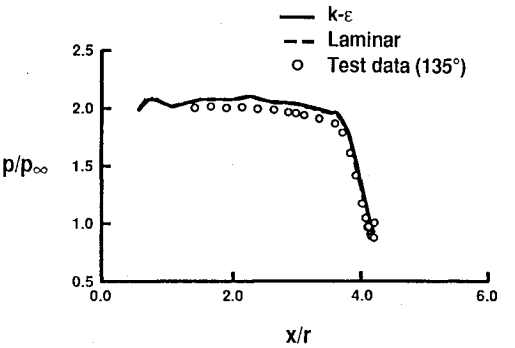

Fig. 8 Pressure comparison for mixed flow turbofan (laminar and k-ε solutions).

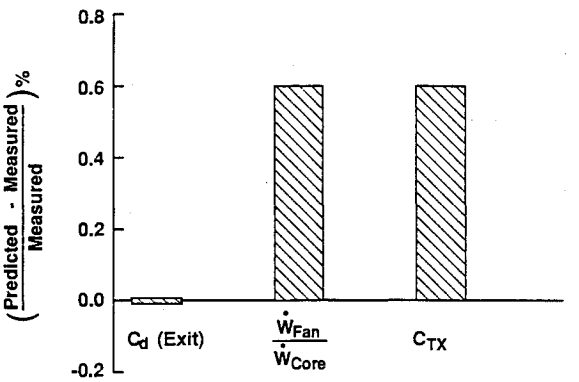

Fig. 9 Validation of mixed flow turbofan performance prediction (k-ε solution).

Concluding Remarks

Predictions of flowfields and performance of separate and mixed-flow turbofan nacelle configurations were accomplished. The flow through the separate flow nacelle geometry produced multishock structures along the plug and core surfaces, as a result of containment by the shear layers between the three flows (i.e., the core, fan, and external streams), and was predicted fairly closely. The separate flow nacelle mass-flow characteristics and axial thrust coefficient was predicted within 0.2% of the experimental data when the k-ε turbulence model was used.

The mixed-flow nacelle mass flow and axial thrust ratio was predicted within 0.1 and 0.6% of the experimental data, respectively. This level of comparison could demonstrate that synergism of the core and fan flows due to mixing was predicted.

The computed solutions provided significant insight into flow details such as shock-shear flow interaction, surface pressures distribution, and the three-dimensional flow generated due to the pylon surface. Detailed comparison of grid effects and laminar and turbulent flow modeling in the solutions indicate that k-ε solutions were more acceptable. It should be considered, though, that the laminar flow calculations required less overall computing resources while producing reasonably acceptable solutions for the cases studied. The present three-dimensional Navier-Stokes code with its different solver options (i.e., laminar and turbulent flow models) can predict pressure distributions and performance quantities for these turbofan nacelle geometries reasonably accurately.

Acknowledgment

The authors would like to express their appreciation to R. R. Babbitt of General Electric Aircraft Engines, who provided test data and configurations for the present paper.

References

[1]Lahti, D. J., Dietrich, D. A., Stockman, N. O., and Faust, G. K., "Application of Computational Methods to the Design of Large Turbofan Engine Nacelles," AIAA Paper 84-0121, Jan. 1984.

[2]Babbit, R. R., Cohn, J. A., and Fleming, K. J., "Advanced High Bypass Mixed-Flow Exhaust System Design Study," AIAA Paper 91-2242, June 1991.

[3]Keith, B. D., Uenishi, K., and Dietrich, D. A., "CFD-Based Three-Dimensional Turbofan Exhaust Nozzle Analysis System," AIAA Paper 91-2478, June 1991.

[4]Ceder, R. D., personal communication, General Electric Aircraft Engines, Cincinnati, OH.

[5]Peery, K. M., and Forester, C. K., "Numerical Simulation of Multistream Nozzle Flows," AIAA Paper 79-1549, July 1991.

[6]Kreskovsky, J. P., Briely, W. R., and McDonald, H., "Investigation of Mixing Turbofan Exhaust Duct, Part I: Analysis and Computational Procedure," *AIAA Journal*, Vol. 22, No. 3, 1984, pp. 374–382.

[7]Chen, H. C., Kusuhose, K., and Yu, N. J., "Flow Simulations for Detailed Nacelle-Exhaust Flow Using Euler Equations," AIAA Paper 85-5003, Oct. 1985.

[8]Brown, J. J., "A Nozzle Design Analysis Technique," AIAA Paper 86-1613, June 1986.

[9]Peace, A. J., "A Method for Calculating Axisymmetric Afterbody Flows," *Journal of Propulsion and Power*, Vol. 13, No. 4, 1987, pp. 357–364.

[10]Thomas, J. L., van Leer, B., and Walters, R. W., "Implicit Flux-Split Schemes for the Euler Equations," AIAA Paper 85-1680, June 1985.

[11]Abdol-Hamid, K. S., "Application of Multiblock/Multizone Code (PAB3D) for the Three-Dimensional Navier-Stokes Equations," AIAA Paper 91-2155, June 1991.

[12]Abdol-Hamid, K. S., Uenishi, K., and Turner, W. M., "A Three-Dimensional Upwinding Navier-Stokes with k-ε Model for Supersonic Flow," AIAA Paper 91-1669, June 1991.

[13]Abdol-Hamid, K. S., Carlson, J. R., and Pao, S. P., "Computational Analysis of Vented Supersonic Exhaust Nozzles Using a Multiblock/Multizone Strategy," AIAA Paper 91-0125, Jan. 1991.

[14]Carlson, J. R., "A Nozzle Internal Performance Prediction Method," NASA TP-3221, Oct. 1992.

[15]Jones, W. P., and Launder, B. E., "The Calculations of Low-Reynolds-Number Phenomena with a Two-Equation Model of Turbulence," *International Journal of Heat Mass Transfer*, Vol. 16, 1973, pp. 1119–1130.